Electronic supplementary information

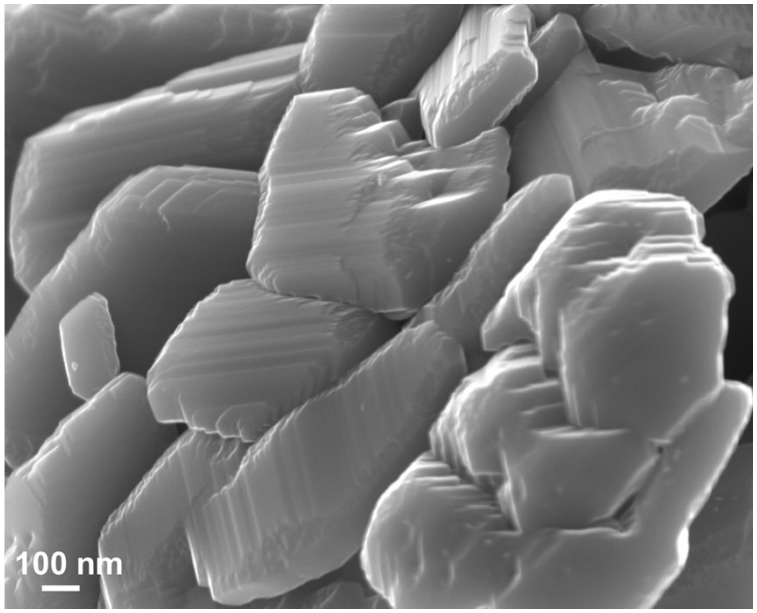

Fig. S1. SEM image of V_2O_5 nanoparticle.

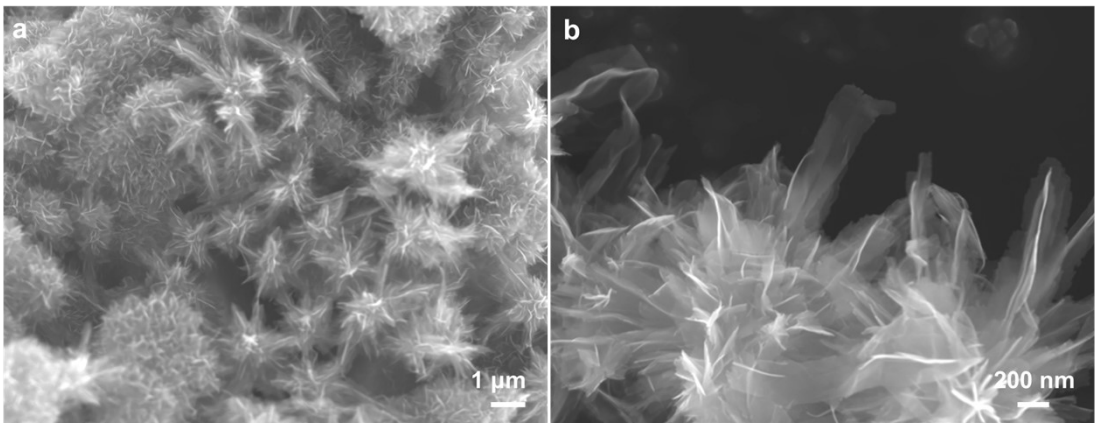

Fig. S2. SEM images of P-VO_x hybrid.

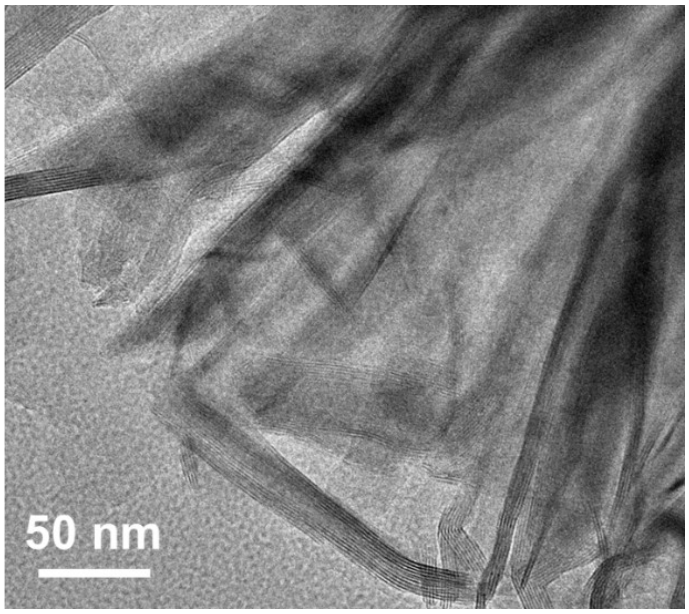

Fig. S3. TEM image of P-VO_x hybrid.

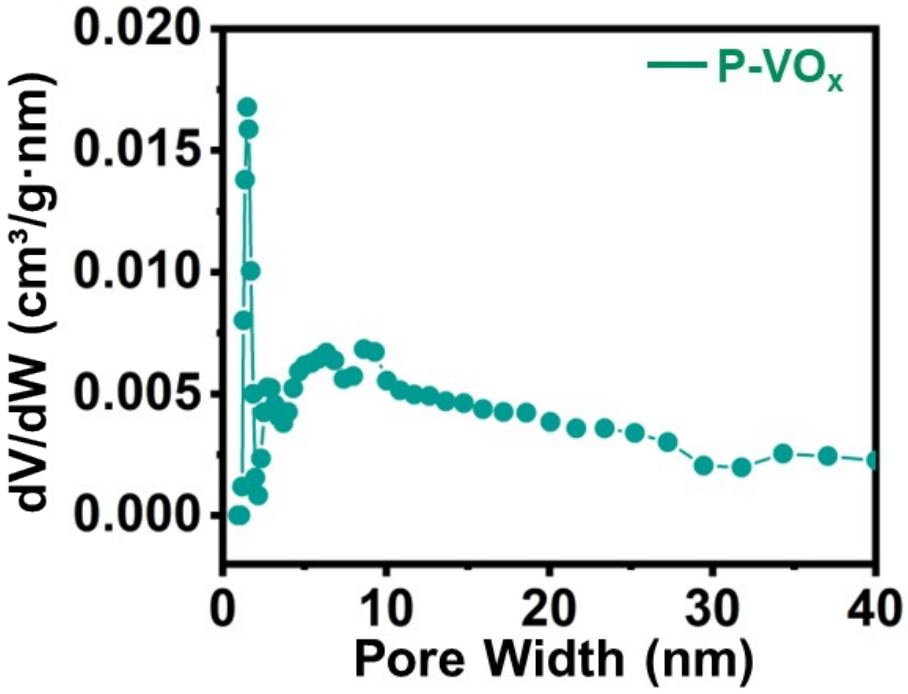

Fig. S4. Pore volume distribution of P-VO_x.

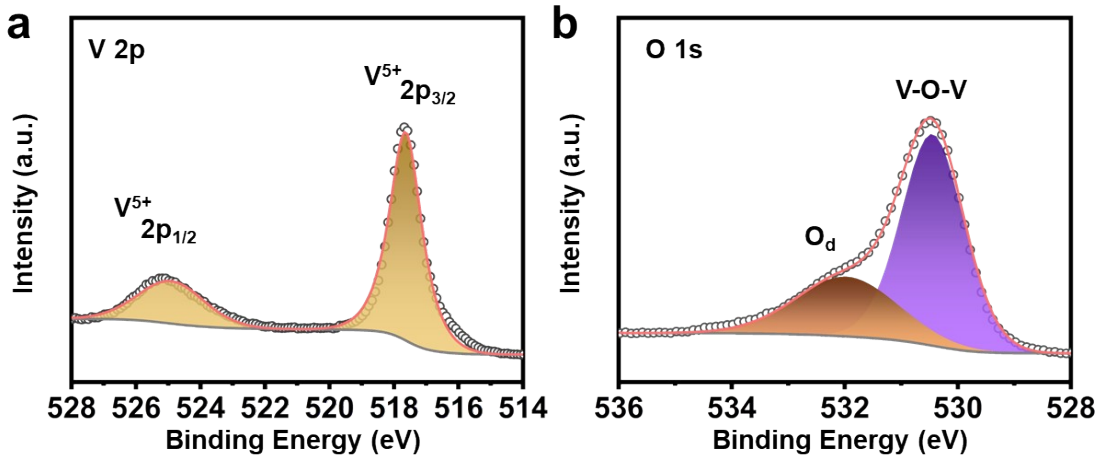

Fig. S5. (a) V 2p and (b) O 1s XPS spectra of V_2O_5 nanoparticle.

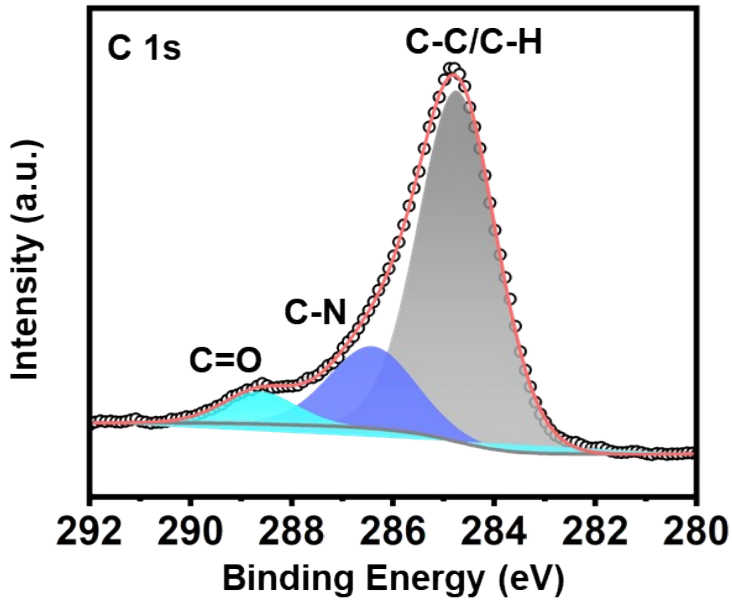

Fig. S6. C 1s XPS spectra of P-VO_x hybrid.

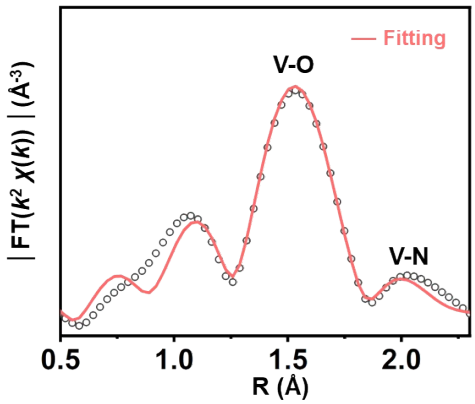

Fig. S7. Quantitative fitting of the V K-edge EXAFS for the P-VO_x sample.

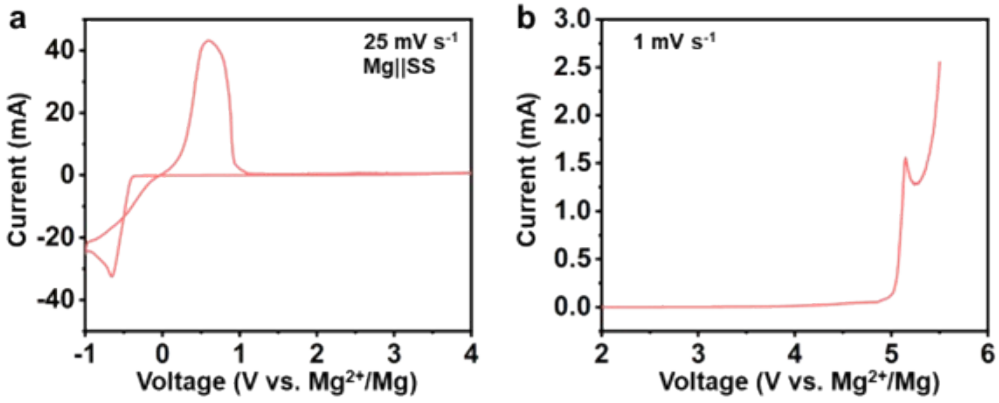

Fig. S8. (a) CV curves of Mg||SS cells at 25 mV s^{-1} with the $Mg[B(HFIP)_4]_2$/DME electrolytes. (b) LSV curves of Mg||GC cells at 1mV s^{-1} with carbon paper current collector as the working electrode substrate.

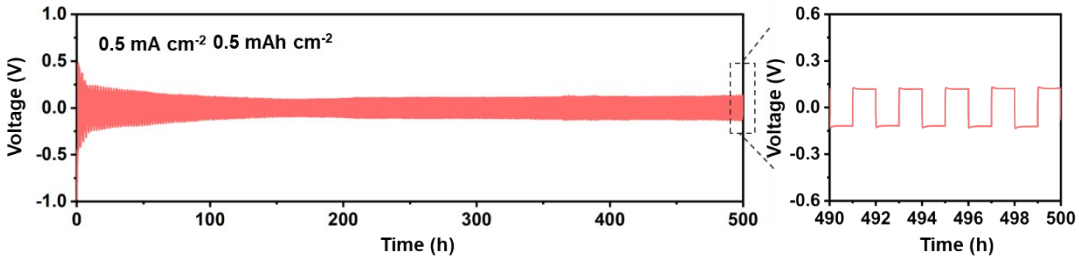

Fig. S9. Cycling performance of Mg||Mg cell at 0.5 mA cm^{-2} with 0.5 mAh cm^{-2}.

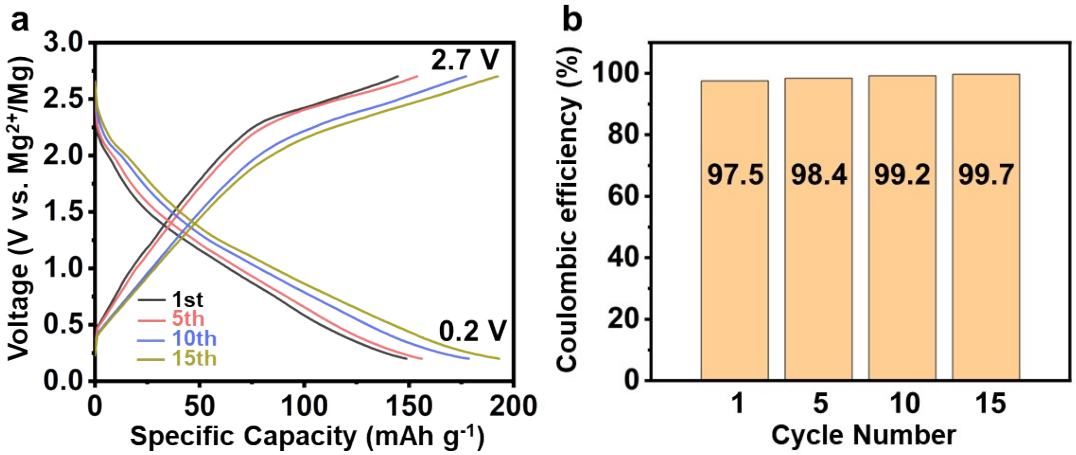

Fig. S10. (a) Charge-discharge curves under different cycles of P-VO_x cathode in RMBs at a current density of 0.1 A g^{-1} within a voltage window of 0.2-2.7 V. (b) Coulombic efficiency under different cycles.

Table S1. The Mg content determined by ICP-OES for P-VO_x at different states.

Samples	Weight of the electrodes (mg)	Weight of active materials (mg)	Constant volume (L)	Mg mass concentration (mg/L)	Mg content (wt%)
Initial discharge	9.2	6.44	0.1	5.4538	8.46
Initial charge	7.4	5.18	0.1	0.9798	1.88
The 10th discharge	12.0	8.4	0.1	9.7258	11.57
The 10th charge	8.4	5.88	0.1	1.8228	3.1

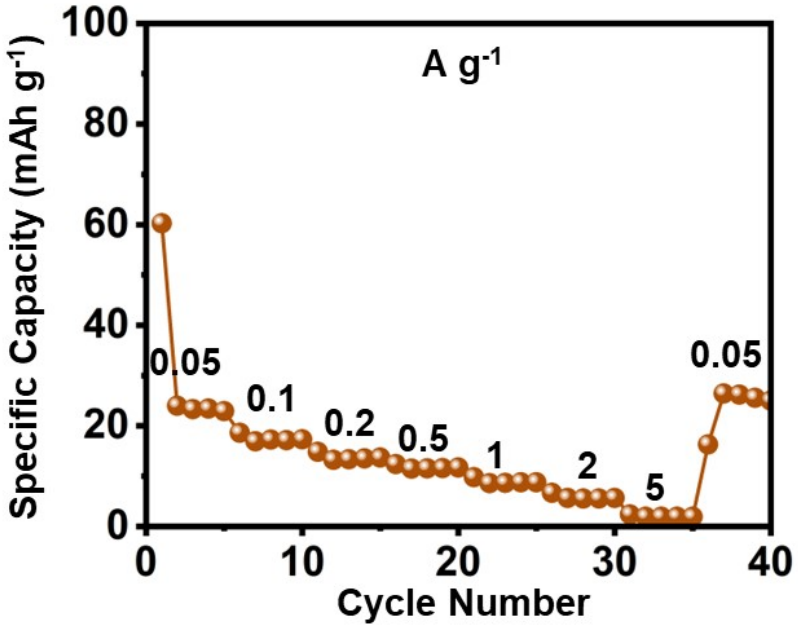

Fig. S11. Rate capability of V_2O_5 nanoparticle.

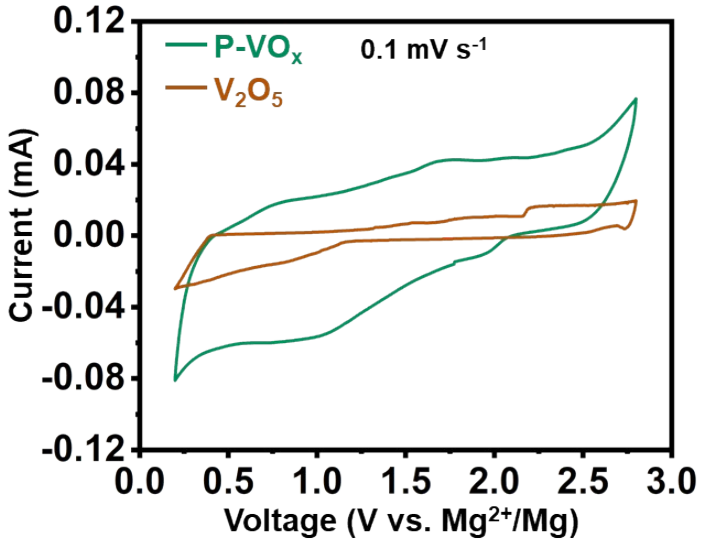

Fig. S12. CV curves of V_2O_5 and P-VO_x cathodes at scan rates of 0.1 mV s^{-1}.

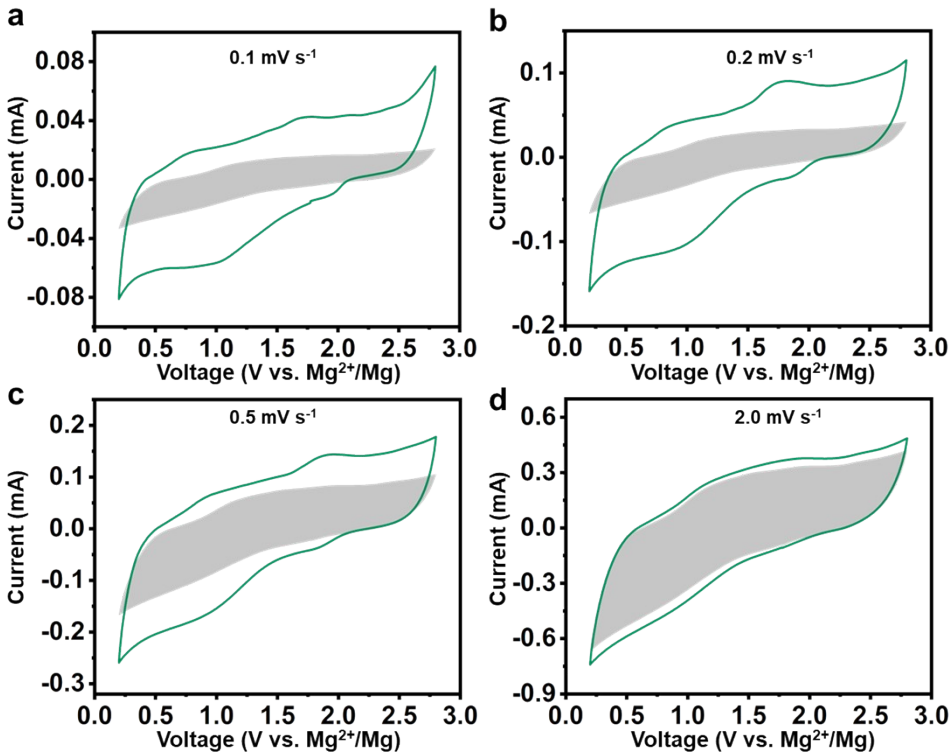

Fig. S13. CV curve of P-VO_x at the scan rate of (a) 0.1 mV s^{-1}, (b) 0.2 mV s^{-1}, (c) 0.5 mV s^{-1} and (d) 2.0 mV s^{-1}. The shaded area represents the capacitive current response ascribed from surface/near surface reaction.

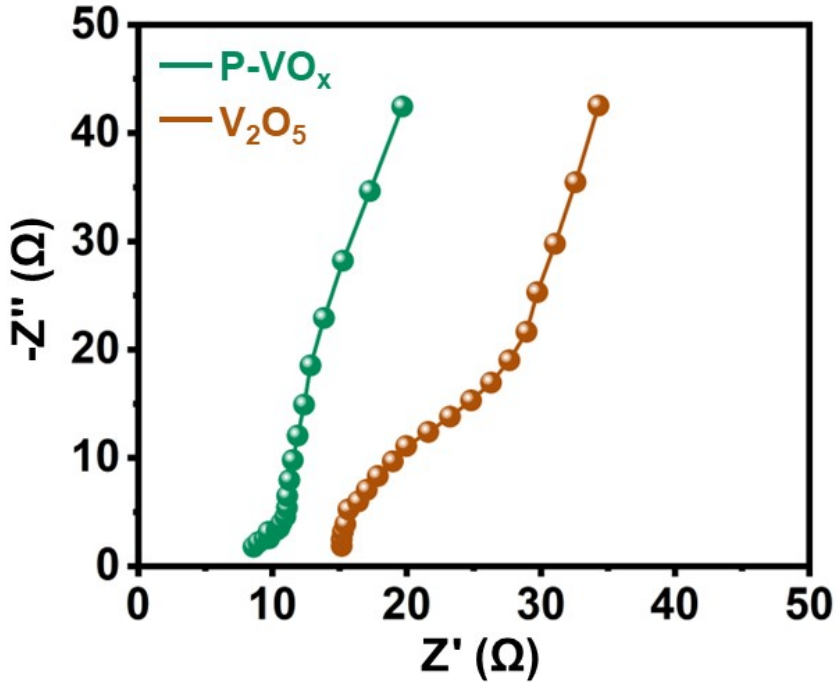

Fig. S14. Nyquist plots of V_2O_5 and P-VO_x initial electrodes.

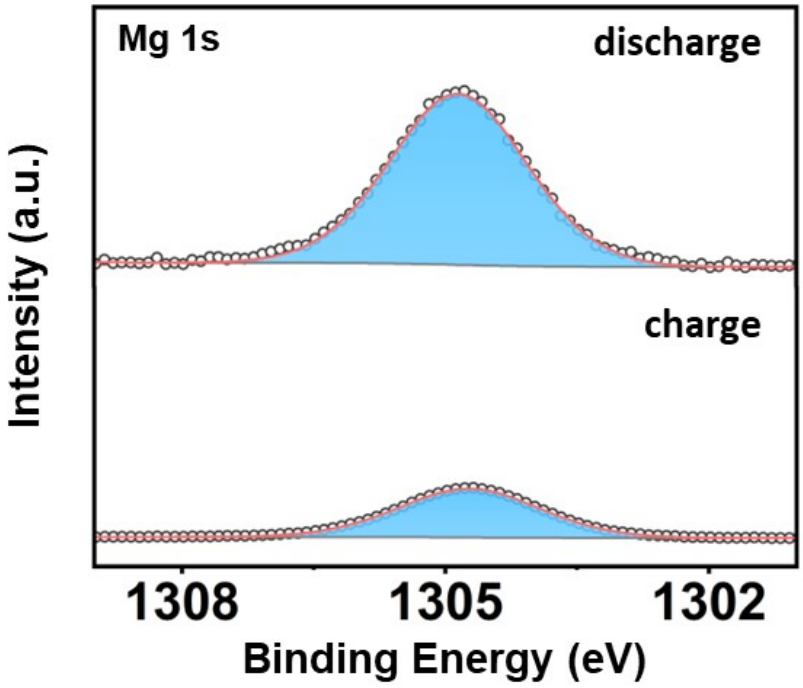

Fig. S15. Mg 1s XPS spectra of P-VO_x electrode in discharged and charged states.

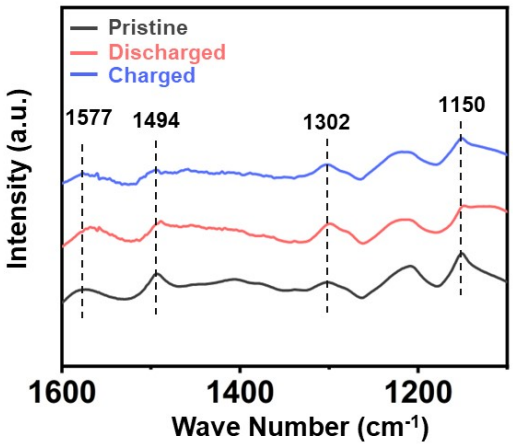

Fig. S16. Ex-situ FTIR of the P-VO_x cathode before and after cycling.

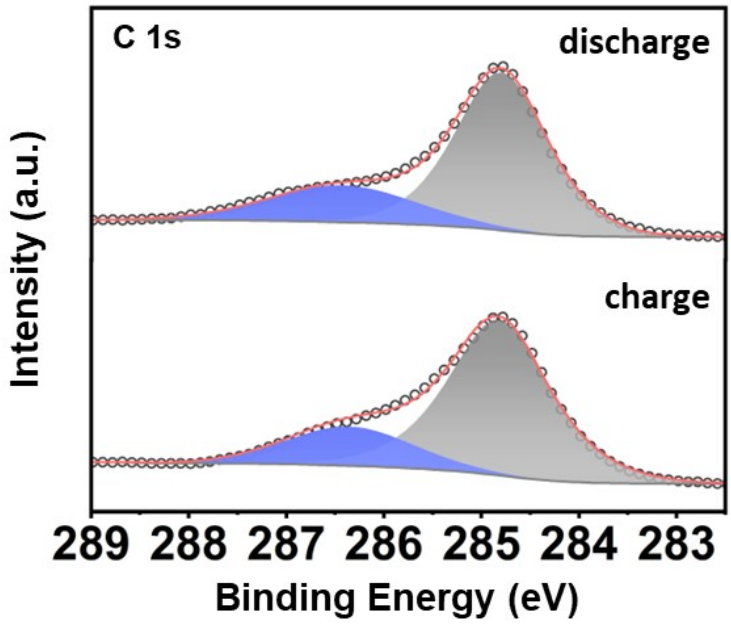

Fig. S17. C 1s XPS spectra of P-VO_x electrode in discharged and charged states.

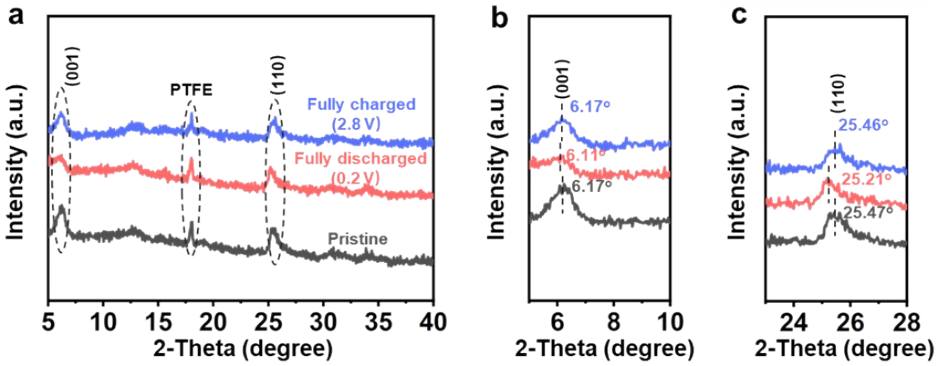

Fig. S18. (a) XRD pattern of P-VO_x electrode under different states. Fine variations of (b) (001) peak and (c) (110) peak.

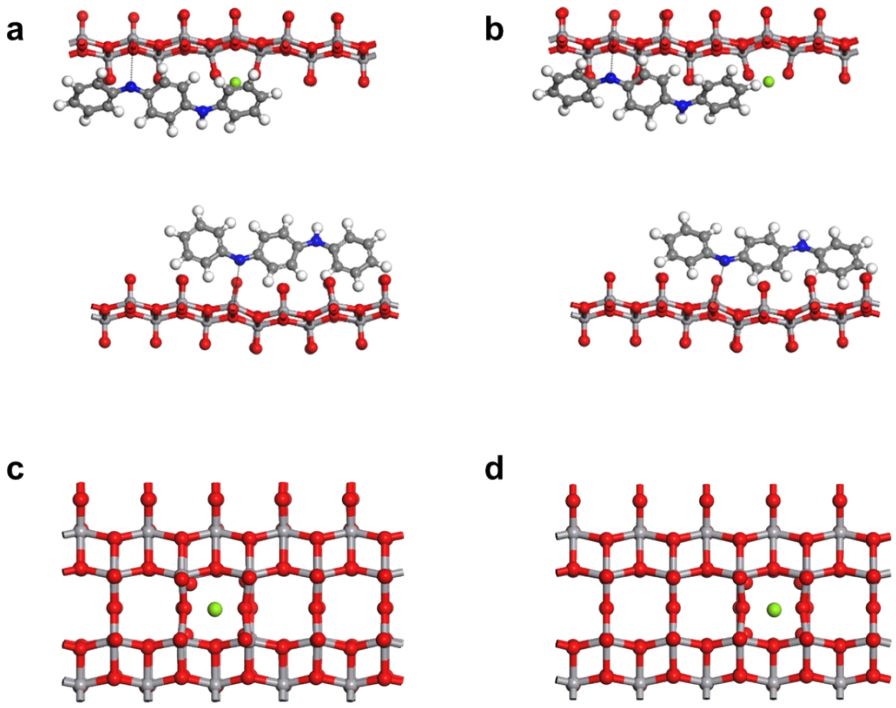

Fig. S19. DFT-calculated (a) initial position and (b) final position of Mg^{2+} along the migration path over P-VO_x. DFT-calculated (c) initial position and (d) final position of Mg^{2+} along the migration path over V_2O_5.